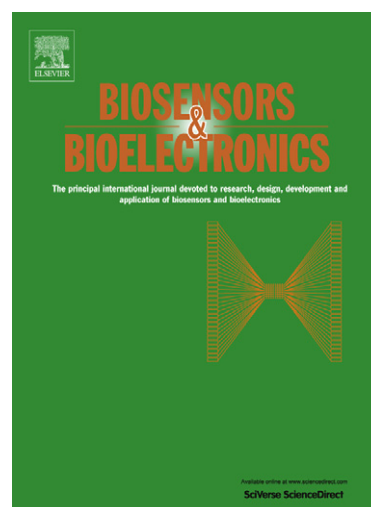




## Author's Accepted Manuscript

Epidermal Tattoo Potentiometric Sodium Sensors with Wireless Signal Transduction for Continuous Non-Invasive Sweat Monitoring

Amay J. Bandodkar, Denise Molinnus, Omar Mirza, Tomás Guinovart, Joshua R. Windmiller, Gabriela Valdés-Ramírez, Francisco J. Andrade, Michael J. Schöning, Joseph Wang



PII: S0956-5663(13)00825-7  
DOI: <http://dx.doi.org/10.1016/j.bios.2013.11.039>  
Reference: BIOS6375

To appear in: *Biosensors and Bioelectronics*

Received date: 24 August 2013  
Revised date: 10 November 2013  
Accepted date: 12 November 2013

Cite this article as: Amay J. Bandodkar, Denise Molinnus, Omar Mirza, Tomás Guinovart, Joshua R. Windmiller, Gabriela Valdés-Ramírez, Francisco J. Andrade, Michael J. Schöning, Joseph Wang, Epidermal Tattoo Potentiometric Sodium Sensors with Wireless Signal Transduction for Continuous Non-Invasive Sweat Monitoring, *Biosensors and Bioelectronics*, <http://dx.doi.org/10.1016/j.bios.2013.11.039>

This is a PDF file of an unedited manuscript that has been accepted for publication. As a service to our customers we are providing this early version of the manuscript. The manuscript will undergo copyediting, typesetting, and review of the resulting galley proof before it is published in its final citable form. Please note that during the production process errors may be discovered which could affect the content, and all legal disclaimers that apply to the journal pertain.

# Epidermal Tattoo Potentiometric Sodium Sensors with Wireless Signal Transduction for Continuous Non-Invasive Sweat Monitoring

Amay J. Bando<sup>a</sup>, Denise Molinnus<sup>a,b</sup>, Omar Mirza<sup>a</sup>, Tomás Guinovart<sup>a,c</sup>, Joshua R. Windmiller<sup>a,d</sup>, Valdes-Ramirez Gabriela Valdés-Ramírez<sup>a</sup>, Francisco J. Andrade<sup>c</sup>, Schoning Michael J. Schöning<sup>b</sup>, Joseph Wang<sup>a\*1</sup>

<sup>a</sup>Department of NanoEngineering, University of California, San Diego La Jolla, CA 92093, USA

<sup>b</sup>Institute of Nano- and Biotechnologies, Aachen University of Applied Sciences, D-52428 Jülich, Germany

<sup>c</sup>Departamento de Química Analítica, Universitat Rovira i Virgili, 43007 Tarragona, Spain

<sup>d</sup>Electrozyme LLC, Executive Square (Suite 485), San Diego, CA 92037, USA

\*Corresponding author. Tel.: +1 858 246 0128; fax: +1 858 534 9553.

josephwang@ucsd.edu

## Abstract

This article describes the fabrication, characterization and application of an epidermal temporary-transfer tattoo-based potentiometric sensor, coupled with a miniaturized wearable wireless transceiver, for real-time monitoring of sodium in the human perspiration. Sodium excreted during perspiration is an excellent marker for electrolyte imbalance and provides valuable information regarding an individual's physical and mental wellbeing. The realization of the new skin-worn non-invasive tattoo-like sensing device has been realized by amalgamating

several state-of-the-art thick film, laser printing, solid-state potentiometry, fluidics and wireless technologies. The resulting tattoo-based potentiometric sodium sensor displays a rapid near-Nernstian response with negligible carryover effects, and good resiliency against various mechanical deformations experienced by the human epidermis. On-body testing of the tattoo sensor coupled to a wireless transceiver during exercise activity demonstrated its ability to continuously monitor sweat sodium dynamics. The real-time sweat sodium concentration was transmitted wirelessly via a body-worn transceiver from the Na-tattoo sensor to a notebook while the subjects perspired on a stationary cycle. The favorable analytical performance along with the wearable nature of the wireless transceiver makes the new epidermal potentiometric sensing system attractive for continuous monitoring the sodium dynamics in human perspiration during diverse activities relevant to the healthcare, fitness, military, healthcare and skin-care domains.

#### Highlights

- Non-invasive epidermal tattoo-based sodium sensor is presented.
- The device is resilient towards mechanical deformations experienced by human epidermis.
- On-body wireless real-time monitoring of sodium dynamics in sweat during physical activity is illustrated.

#### Keywords

Sweat Sodium, Screen Printing, Epidermal Electronics, Wireless Electronics, Ion selective electrode

## 1. Introduction

Wearable chemical sensors, capable of real-time on-body monitoring of chemical constituents, can yield significant additional insights into the overall health status and performance of individuals, compared to that obtained by monitoring physical variables alone (Morris et al., 2008). Roger's group introduced epidermal sensors for measuring physical physiological parameters (Kim et al., 2011). Electrochemical devices offer considerable promise for such continuous non-invasive on-body monitoring (Windmiller et al., 2012). Particular attention has been given recently to printed electrochemical sensors on flexible substrates and textiles (Windmiller and Wang, 2013). Recently our group introduced the first tattoo-like electrochemical sensors, capable of adhering and conforming to the epidermis, for amperometric biosensing of lactate in human perspiration (Jia et al., 2013a) or potentiometric sensing of sweat pH (Bandodkar et al., 2013a) and ammonium (Guinovart et al., 2013a). Continuous monitoring of sweat lactate and pH dynamic during exercise events has thus been demonstrated. Extending this attractive platform towards continuous non-invasive monitoring of key sweat electrolytes should benefit diverse healthcare, fitness, and military applications.

The present article describes the design and analytical performance of a temporary-transfer tattoo solid-contact ion-selective electrode (ISE) for the continuous non-invasive monitoring of sweat sodium concentration directly on the human epidermis. Sodium is the most abundant electrolyte present in human sweat (Harvey et al., 2010). It is an excellent marker for electrolyte imbalance and provides valuable information regarding an individual's physical and mental wellbeing. Replenishing the sodium level in the body is important since it is essential for regulating water balance, pH, and osmotic pressure. This is especially true for athletes (Rosner and Kirven, 2007), people working in hot and humid environments (Ladell, 1955) and patients suffering from Cystic Fibrosis (Stern, 1997), since, in these cases, the amount of sodium lost via sweating can reach dangerously high levels causing hyponatremia, leading to deleterious physiological conditions (Speedy et al., 2001). Monitoring the amount of sodium loss during sweating is thus extremely important (Schazmann et al., 2010). A wearable device quantifying in real-time the transient sweat sodium concentrations could alert the wearer regarding his electrolyte loss and the concomitant need for electrolyte replenishment. Such device must be compact, easily worn, autonomous, and able to generate, display or store the results in a continuous fashion.

The current methodology for estimating sodium in the perspiration relies on collecting sweat via Macroduct<sup>®</sup> sweat collection systems followed by lab-based analysis of the collected fluid (Lee et al., 2010). However, such a protocol has several shortcomings for routine operation (Schazmann et al., 2010). These include (i) A large sweat collection system that is uncomfortable to wear thus hindering the wearer's routine. (ii) Bulky centralized expensive instrumentation for sweat analysis that is incompatible with on-body testing. (iii) Compromised accuracy due to evaporation of the sweat samples during their transport. Such drawbacks can be addressed using wearable sensors. Diamond's team demonstrated a wearable waistband sodium sensor for on-

body potentiometric monitoring of sodium (Schazmann et al., 2010). Additional efforts aimed at on-body monitoring of other electrolytes included measurements of sweat chloride (Ruiz et al., 2009), ammonium (Guinovart et al., 2013a), potassium (Guinovart et al., 2013b) and pH (Bandodkar et al., 2013) in human perspiration using disposable strip, textile-based, and tattoo-like ISE, respectively. Parallel activity has been devoted lately towards the development of portable wireless transceivers for potentiometric sensors (Novell et al., 2013; Fay et al., 2011). However these devices have not been applied for on-body electrolyte monitoring.

In the following sections we will describe the design and fabrication of the new epidermal tattoo sodium ISE sensor, along with detailed *in-vitro* characterization of the analytical behavior and mechanical resiliency, followed by on-body testing using healthy individuals during exercise activity in conjunction with the wireless signal transduction. The new skin-worn sodium sensing system has been fabricated by combining thick film, laser printing, solid state potentiometry, fluidics and tattoo-transfer technologies (**Fig. 1**). In accordance to the phase-boundary potential theory (Bakker, 2010), the response of the new tattoo sodium sensor depends on the charge separations between the organic phase (membrane) and the aqueous phase (sample). The ionophore-based flexible solid-state Na ISE has been paired with a custom-designed Bluetooth-enabled wireless wearable transceiver, embedded in an adjustable armband, for continuous monitoring of sweat sodium levels directly on the human epidermis. The attractive performance and features of the new sodium tattoo-ISE indicate considerable promise for diverse real-life on-body monitoring applications.

## 2. Material and methods

### 2.1. Reagents

Selectophore™ grade sodium ionophore X, Bis(2-ethylhexyl) sebacate (DOS), sodium tetrakis[3,5-bis(trifluoromethyl)phenyl]borate (Na-TFPB), polyvinyl chloride (PVC), tetrahydrofuran (THF), and sodium chloride (NaCl), sodium sulfate (Na<sub>2</sub>SO<sub>4</sub>), sodium bicarbonate (NaHCO<sub>3</sub>), potassium chloride (KCl), magnesium chloride (MgCl<sub>2</sub>·6H<sub>2</sub>O), sodium phosphate anhydrous monobasic (NaH<sub>2</sub>PO<sub>4</sub>), calcium carbonate (CaCO<sub>3</sub>) and ammonium hydroxide (NH<sub>4</sub>OH) were procured from Sigma Aldrich (St. Louis, MO). Polyvinyl butyral resin BUTVAR® B-98 (PVB) was obtained from Quimidroga (Spain). All reagents were used without further purification. Carbon fibers (8 μm diameter, 6.4 mm length, 93% purity) were purchased from Alfa Aesar (Ward Hill, MA) and further processing was performed to reduce their length to approximately 2 mm; subsequent cleaning in acetone was performed. Ultrapure water was employed in all of the investigations. Chopped carbon fibers were dispersed within both conductive carbon (E3449) and silver/silver chloride (Ag/AgCl) (E2414) inks (Ercon, Inc, Wareham, MA). The carbon fibers were added to these inks, at 1.5% w/w and 1.2% w/w, respectively, to increase the tensile strength of the printed electrodes. Transparent insulator ink

(DuPont 5036) was purchased from DuPont (Wilmington, DE). The stencil patterns were designed in AutoCAD (Autodesk, San Rafael, CA) and outsourced for fabrication (Metal Etch Services, San Marcos, CA). Laser temporary transfer tattoo paper kits were obtained from HPS Papilio (Rhome, TX). Artificial sweat comprised of various potential interfering electrolytes, including NaCl, Na<sub>2</sub>SO<sub>4</sub>, NaHCO<sub>3</sub>, KCl, NaCl, MgCl<sub>2</sub>·6H<sub>2</sub>O, NaH<sub>2</sub>PO<sub>4</sub>, CaCO<sub>3</sub> and NH<sub>4</sub>OH at physiological concentrations (Harvey et al., 2010).

## 2.2. Instruments

Screen printing was performed using an MPM-SPM semi-automatic screen printer (Speedline Technologies, Franklin, MA). Electrochemical characterization was performed at room temperature leveraging a CH Instruments (Austin, TX) model 630C electrochemical analyzer or a wireless transceiver. Mechanical stress studies were performed using a tensile test machine (Instron® 5900 Series Model 5982, Norwood, MA). The wireless transceiver was custom designed. Details on design and fabrication of wireless transceiver are given in Section S.1 of the Supplementary Data Section. Briefly, the transceiver consisted of an electrochemical analyzer-on-a-chip, an 8-bit low-power microcontroller (MCU, running custom scripts to perform the electrochemical measurements), a Bluetooth v2.1 + EDR 2.4GHz wireless module, voltage regulator, USB battery charger IC, and all associated passive components mounted on a 30 mm x 45 mm printed circuit board (PCB) and was powered by a rechargeable Li-ion 2032 button-cell battery (recharged via a micro-USB connector used for flashing the MCU). Data was relayed at one-second intervals to a Bluetooth-enabled PC via a serial data stream. A spring-loaded pressure connector was leveraged in order to interface with the Na-tattoo epidermal sensor

## 2.3. Tattoo Fabrication, Modification and Transfer Process

The Na-tattoo pattern was superimposed on a laser-printed color rendering of an artistic “Tiger Face”. The first step consisted of screen printing of a layer of the transparent insulator onto the entire tattoo base paper sheet. This was followed by laser printing a two dimensional array of the “Tiger Face” onto the insulator-coated tattoo base paper. Subsequently, a layer of commercial skin-color paint was printed over the entire tattoo sheet and was allowed to dry at room temperature for 2 h. The next steps involved printing the carbon indicator and Ag/AgCl reference electrodes, followed by printing a layer of transparent insulator ink to define the electrode area and contact pads. The contacts for interfacing the Na-tattoo sensor to either the electrochemical analyzer or the wireless transceiver were fabricated via screen printing carbon ink on a flexible polyethylene terephthalate (PET) substrate. The printing process for electrodes and PET contacts has been described earlier (Jia et al., 2013a; Bhandodkar et al., 2013b). Thereafter, the region of the PET in contact with the Na-tattoo sensor was completely sealed by a clear nail varnish. This was necessary to avoid the accumulation of sweat in the seams.

The sodium selective membrane cocktail composition consisted of 1 mg sodium ionophore X, 0.55 mg Na-TFPB, 33 mg PVC, and 65.45 mg DOS dissolved in 660  $\mu\text{L}$  of nitrogen-purged THF. The cocktail was thoroughly mixed to dissolve all the components. The reference cocktail was prepared by dissolving 78.1 mg PVB and 50 mg NaCl in 1 mL methanol. The PVB membrane has been recently described (Guinovart et al., 2013a). Briefly, the polymeric PVB membrane, containing electrolytes forms a nanoporous structure that allows the exchange of electrolytes with the solution, providing a stable potential, insensitive to changes in the ion concentration over a large concentration range (Guinovart et al., submitted). To build the sensor, 10  $\mu\text{L}$  of the sodium selective membrane cocktail was drop-casted onto the carbon indicator electrode and the reference electrode was modified by 4  $\mu\text{L}$  of the reference cocktail. The modified Na-tattoos were left to dry overnight before their implementation in any of the studies.

During *in-vitro* studies, the Na-tattoo was applied to rigid and elastic substrates in a similar fashion as described earlier (Jia et al., 2013b). In case of epidermal evaluation of the Na-tattoos, a fluidic channel and sink (*stick-on fluidic channel*) was fabricated atop the Na-tattoo [Fabrication and photograph of *stick-on fluidic channel* are given in Section S.2 and Fig. S1 of Supplementary Data Section]. The *stick-on fluidic channel* directed the sweat to first flow over the two electrodes and then to the sink. In order to apply the Na-tattoo to the epidermis, an inverted U-shaped adhesive layer was applied to the skin. The gap present in the U-shaped adhesive was included for facilitating the replenishment of perspiration over the two electrodes (Jia et al., 2013a). Thereafter, the transparent protective film present on the *stick-on fluidic channel* (attached to the Na-tattoo) was gently peeled and applied to the aforementioned U-shaped adhesive layer. For continuous sodium monitoring, the user first applies the tattoo sensor, as was described earlier (Jia et al., 2013a) followed by wearing of wireless transceiver such that its contact pads are aligned with that of the Na-tattoo. The data is then wirelessly transmitted to a notebook for logging and display. The complete fabrication and application of the Na-tattoo ISE to the epidermis is shown in **Fig. 1**. A top view of the tattoo with the dimensions of the individual electrodes is shown in **Fig. S2**.

#### 2.4. *In-vitro* Evaluation of the Na-Tattoo Sensors

The preliminary *in-vitro* studies for the Na-tattoo sensors were carried out by using a CH Instruments electrochemical analyzer. The Na-ISE tattoos were applied to rigid plastic substrates to evaluate the change in electromotive force (EMF) across the two electrodes in the presence of different concentrations of NaCl solutions. A similar study was also performed using artificial sweat. Furthermore, a carry-over study was conducted to check reversibility of the Na-tattoo sensors. In this experiment, the Na-tattoo ISE was exposed to NaCl solutions whose concentration alternated between 0.1mM and 10mM. The long term storage stability of the Na-tattoo was examined for a period of 3 weeks using 6 different electrodes. During this period, the sensors were kept in ambient conditions and no special effort was taken to protect these devices from light, dust and other environmental conditions that could be detrimental to the sensor response. In a separate set of studies, Na-tattoo sensors were applied to a Gore-tex<sup>TM</sup> fabric to

analyze the effect of mechanical deformation on sensor response. Subsequently, they were subjected to various mechanical deformation permutations by repeatedly bending, stretching and poking the tattoos on a tensile test machine. During the bending/stretching studies, the Na-tattoo sensor was fixed between two vertical clamps that moved at a predefined speed of 2 mm/s. In the bending study, the Na-tattoo was bent repetitively by  $180^{\circ}$  for a total of 100 cycles and the potentiometric response was recorded after every 20<sup>th</sup> bending iteration. In case of stretching studies, the Na-tattoo sensor was subject to increasing strain from 0 to a maximum of 26%. The strain was increased after every 20 fatigue cycles for a total of 80 cycles. Similar to the bending study, the Na-tattoo response was measured after every 20 cycles. The poking evaluation on the Na-tattoo sensor consisted of clamping the device to a horizontal mounting stage. The sensor was then repetitively indented to a depth of 5 mm by a cylindrical probe. The sensor's response was recorded at an interval of 10 poking (indentation) iterations. The effect of temperature variation on tattoo response was also studied over the  $30^{\circ}\text{C}$  -  $40^{\circ}\text{C}$  range. The study was performed by incubating the tattoo sensors in varying NaCl solutions at various temperatures.

### 2.5. Epidermal Na-Tattoo Sensor Studies

Epidermal evaluation of the Na-tattoo sensor was performed on ten healthy consenting subjects (between the ages of 20 and 40 years) with no prior history of heart conditions, diabetes, or chronic skeletal muscular pain. The subjects were recruited in response to follow-up from flyers posted within the university. Prior to the study, the subjects were prescreened and a signed consent form was obtained from each individual. The study was performed in strict compliance with the protocol that was approved by the institutional review board (IRB) at the University of California, San Diego. The study was deemed by the IRB as posing “*no greater than minimal risk*”. Preceding an on-body test, the Na-tattoo sensor was calibrated with standard NaCl solutions (1, 10 and 100 mM) at  $37^{\circ}\text{C}$ . The exercise bout consisted of cycling on a stationary cycle for 30 min followed by a 3 min of cool-down session and another 3 min of complete rest while remaining on the stationary cycle. Ramp mode was selected to insure that subjects perspired during the study. In this mode, the resistance increased every 3 min for the first 21 min followed by a gradual decrease. The absolute resistance level was selected according to subject's fitness level while the same intensity profile was employed throughout the human studies. However, in some cases (involving subjects who took more time to perspire), the exercise bout was extended beyond 30 min. Firstly, the Na-tattoo was evaluated for its performance in real-life situation by applying the Na-tattoo to five random participants and interfacing it with the electrochemical analyzer. The real-time data was collected and logged using the CH instrument software. Upon validating the Na-tattoo response, the next sub-section of the epidermal study consisted of integration of the Na-tattoo sensor with the wireless transceiver. Before using the wireless transceiver in any human trials, it was first characterized in-vitro for its ability to seamlessly transmit data from the Na-tattoo to a laptop. For this study, a Na-tattoo sensor was applied to a rigid plastic substrate (as discussed in Section 2.4) followed by coupling it to the wireless transceiver. The device was tested by performing calibration and hysteresis studies (as

discussed in Section 2.4). During these studies the wireless transceiver transmitted real-time data from the Na-tattoo sensor to a laptop via Bluetooth. Upon completion of its in-vitro evaluation, the transceiver was used for on-body studies. This was achieved by applying the Na-tattoo sensor to the remaining five subjects along with the wireless transceiver. In these cases the data was seamlessly transmitted from the Na-tattoo sensor to a laptop by the wireless transceiver while the subjects perspired on the stationary cycle.

### 3. Results and Discussion

#### 3.1. In-vitro Na-tattoo Sensor Characterization Studies

The composition of the ion selective and reference membranes has been optimized to approach a Nernstian response towards the primary sodium ion while mitigating potential sources of interference. The optimized sodium selective membrane cocktail composition comprised of 1 mg sodium ionophore X, 0.55 mg Na-TFPB, 33 mg PVC, and 65.45 mg DOS dissolved in 660  $\mu\text{L}$  of nitrogen-purged THF. Upon using this composition, the sensor responded instantaneously in a near-Nernstian fashion to varying sodium concentrations over the 0.1 to 100 mM range (slope: 63.75 mV/ $\log_{10}[\text{Na}^+]$ , R.S.D.: 5.77%,  $n = 6$ ). **Fig. 2A** displays a typical response of the Na-tattoo sensor obtained during this study. The EMF versus  $\log_{10}[\text{Na}^+]$  plot reveals that the signal reaches steady-state within 10 s. Such a rapid response is essential for epidermal sensors, aimed at monitoring rapidly changing sodium sweat levels. The long term stability of the Na-tattoos was also studied over a period of three weeks using 6 different tattoo sensors (Supplementary information, **Fig. S3**). It was observed that the Na-tattoo maintained its fast response towards sodium ions with minimal loss in its sensitivity (slope: 60.41 mV/ $\log_{10}[\text{Na}^+]$ ; R.S.D.: 5.71%;  $n = 6$ ) even when kept in the ambient conditions, without any protection from light, moisture and dust. This reflects the resiliency of the Na-tattoos sensor against degradation and indicates that the device requires no special storage conditions. While an offset was observed for all sensors after the three week study, this could be readily addressed by calibrating each sensor prior to its on-body testing, thus ensuring reliable data. Furthermore, a long-term drift of 2.8 mV/h was recorded for the Na-tattoos.

The human sweat contains several interfering electrolytes such as potassium, calcium, magnesium, and ammonium (Harvey et al., 2010). Thus, it is essential that epidermal sodium sensors perform desirably in the presence of these electrolytes. The selectivity of the Na-tattoo sensor was evaluated in artificial sweat containing physiological levels of potentially interfering electrolytes, while varying the sodium concentration over the physiological range (up to 110 mM) (Bates and Miller, 2008). The response displayed in **Fig. 2B**, demonstrates the Na-tattoo sensor response in artificial sweat. The Na-tattoo sensor displayed a potential drift (in the artificial sweat) of 4.2 mV/min, which can be minimized by further surface modification of the electrode (Fibbioli et al., 2000).

Fast reversible interaction between the sensor and the analyte solution is mandatory for obtaining Nernstian response (Buck, 1978). The sweat sodium concentration commonly fluctuates with sweat rate (Buono et al., 2007; Sato et al., 1989). Hence, a reversible and rapid response is an essential requirement for a wearable device for monitoring the dynamics of sweat sodium levels. The reversibility of the Na-tattoo sensor was examined by measuring its response to alternating 0.1, 1 and 10 mM NaCl solutions, using 6 such carry-over cycles over a 4 min period. As illustrated in **Fig. 2C**, the Na-tattoo sensor displays a nearly-reversible response in the millimolar range. The sensor requires a slightly longer response time for the 0.1mM concentration; this should not affect the sensor performance in real-life scenarios since sodium sweat concentrations are commonly in the millimolar range.

Apart from its ability to accurately detect sodium, the new epidermal ISE must also be able to withstand the rigors of daily human wear. Strain caused due to mechanical deformations, experienced by the epidermis during physical activity, can have deleterious effect on the sensor performance. Therefore, the effect of such strains on the Na-tattoo response was evaluated. The sensor was bent repeatedly by  $180^\circ$  and its response was measured after every 20 fatigue cycles. **Fig. 3A** displays the response of the sensor in connection to 100 such bending cycles, while the inset shows a photograph illustrating the extent of mechanical deformation witnessed by the tattoo during this study. Nearly identical calibration plots are observed after each 20 bending cycles (R.S.D.=6.83%), clearly demonstrating that the Na-tattoo ISE can withstand  $180^\circ$  repeated bending strain – the maximum a human body can withstand – with only negligible change in its response. Stretching is another strain that the epidermal sensor may experience. The human arm tissue can endure an ultimate failure strain of about 27% (Jacquemoud et al., 2007; Gallagher et al., 2012), beyond which the tissue ruptures leading to injury. The Na-tattoo sensors were designed to survive such extreme conditions too. As illustrated in **Fig. 3B**, the Na-tattoo signal is quite stable even when a stretching strain of 26% is applied to the underlying Gore-Tex<sup>®</sup> substrate. The R.S.D. value for the entire study of 80 stretching cycles was 9.35%. The inset of **Fig. 3B** shows an image of a stretched Na-tattoo sensor. It was noticed that when the underlying Gore-Tex<sup>®</sup> substrate is stretched, the Na-tattoo sensor first stretches with the substrate and on further increasing the strain, it generates corrugates within the tattoo structure to accommodate the excess stress. As a result, minimal tensile stress is experienced by the Na-tattoo sensor. The tattoo can thus withstand such high strains without compromising its sensing properties. Epidermal sensors can also experience mechanical deformations due to indentations caused by poking. The response of the Na-tattoo sensor was evaluated against such deformations. The tattoo was thus repeatedly indented to a depth of 5mm with a cylindrical probe and the response was measured after every 10 indentations. As illustrated in **Fig. 3C**, this study led to a relatively higher R.S.D. of 13%. Such behavior reflects the damage caused by the sharp edges of the cylindrical probe (used for inducing the dents) and not due to the dents themselves. It should be pointed out that such harsh indentations are rarely experienced by the epidermis. Overall, the mechanical deformation studies performed on the Na-tattoos sensor reveal that they maintain their favorable potentiometric response under extreme mechanical stress. We also evaluated the

dependence of the Na-tattoo response on the temperature over the 30<sup>0</sup>C - 40<sup>0</sup>C range. Such range reflects the temperature variation of the human skin (Rowell et al., 1969). As illustrated in **Fig S4**, a small variation in slope of 0.1% was observed.

### 3.2. On-Body Characterization of the Na-Tattoo Sensor

Preliminary epidermal evaluation of the Na-tattoo was performed by repeatedly pinching and poking the tattoo sensor applied to the deltoid of a human subject (**Fig. S5, Supplementary Data**). Visual analysis showed that such deformations have negligible effect on its structural integrity. Subsequently, ten human subjects were recruited for evaluating the on-body performance of the new ISE device. During this study, the tattoo sensor was applied to the right deltoid of each participant. The ability of the sensor for real-time epidermal monitoring of sodium levels in sweat was first examined by interfacing the skin-worn Na-tattoo sensor with a conventional electrochemical analyzer, in a manner similar to our earlier work (Jia et al., 2013a). Five subjects were randomly selected to participate in this sub-section of the epidermal study. For each case, the lack of sweat at the beginning of the exercise bout led to random fluctuating open-circuit potentials corresponding to sodium concentration well beyond the physiological range. The data measured during this phase is irrelevant and must be neglected due to the incompleteness of the electrochemical cell. However, the sweat formation leads to completion of the cell and to stabilization of the potential measured. The potential measured after this point corresponded to physiologically-relevant sodium concentrations (Bates and Miller, 2008). **Fig. 4A and 4B** display representative real-time sodium concentration profiles obtained during this study for two different subjects. Note that these tracings do not show the initially random physiologically-irrelevant values recorded before sweating. In most cases, the initial random fluctuating data was followed by a dip in the measured potential when the subject began perspiring (as observed in **Fig. 4A** and more prominently in **Fig. 4B**). The exact reason for this phenomenon is being investigated. Physiologically relevant data was obtained after this point since the fluctuating data before this dip has no physiological relevance. In case of each subject, it was noticed that just the initial glazing of the skin due to sweat formation was sufficient to obtain physiologically relevant data. This can be attributed to the property of the *stick-on fluidic channel* to efficiently direct low amounts of sweat to the two electrodes and thus underscores the ability of the Na-tattoo sensor to detect sodium even during minimal sweating. This is an important feature of the Na-tattoo sensor, particularly for wearers with low sweat rate. As mentioned earlier, the exercise bout involved increasing the intensity level after every 3 min. Due to this incremental mode of workout, the perspiration rate increased with time. Several groups have shown that the sodium concentration in the perspiration increases with increasing

sweat rate (Buono et al., 2007; Sato et al., 1989). Indeed, a similar trend was observed during the epidermal studies. **Fig. 4A and 4B** clearly demonstrates the expected increasing sodium concentration with the course of the study. The study substantiated the ability of the Na-tattoo to respond to the temporal sodium level in human perspiration. It should be noted that although the overall trend was similar for the different subjects, they display distinct temporal sodium profiles. This could be attributed to variety of factors, such as an individual's genetic predisposition (Bank et al., 1978; Eichner, 2008), diet (Sigal and Dobson, 1968), environmental conditions (Bates and Miller, 2008; Taylor et al., 1943) and heat acclimatization (Allan and Wilson, 1971). Furthermore, although the subjects used a similar exercise routine, each cycled at his own comfortable speed.

The subsequent phase of the epidermal study involved implementing a custom-designed wireless transceiver (details of design and fabrication is discussed in Section 2.2) to relay the real-time potentiometric data generated at the Na-tattoo sensor to a personal computer. Briefly, it consisted of an electrochemical analyzer-on-a-chip, a low-power microcontroller, a Bluetooth wireless module, voltage regulator, USB battery charger IC, on a 30 mm x 45 mm printed circuit board, and was powered by a rechargeable button-cell battery. The wireless transceiver was first evaluated in-vitro by coupling it with a Na-tattoo sensor. Its transduction characteristics were evaluated by performing calibration and carry-over studies (**Fig. 5**). During these studies, it was noted that the wireless device seamlessly transmitted the analytical data over a distance of 10 m from the Na-tattoo sensor to a notebook for over an hour of use. Well defined calibration plot (slope: 64.1 mV/log<sub>10</sub>[Na<sup>+</sup>]) with minimal carry over effects are indicated from **Fig. 5A and 5B**, respectively. Furthermore, the response of the Na-tattoo sensor was similar to that obtained from the desktop electrochemical analyzer, substantiating the analytical fidelity of the wireless transceiver. For its epidermal evaluation, the Na-tattoo sensor and the wireless device were adorned by each of the remaining five subjects, as shown in **Fig 6A**. The inset displays a close-up of the entire device. **Fig. 6B** displays an image of the wireless transceiver encapsulated in the pocket of an armband while the inset shows the unpackaged system along with a US quarter dollar coin for size comparison. An identical workout regimen (as discussed above) was used in this phase of the epidermal study. **Fig. 6C and D** displays the transient sweat sodium response for two subjects. The exact reason for the sudden jump observed in **Fig. 6C** at around 1600 s is unclear. However, as mentioned earlier each subject has a unique sodium profile. Note that these tracings do not show the initially recorded values before sweating. An overall increment in the sodium concentration was recorded by the wireless transceiver during the entire course of the exercise bout. The overall trend was comparable to the profile obtained with the conventional electrochemical analyzer. Furthermore, the wireless transceiver obviated the need for connectors and thus greatly reduced the intrusiveness of the analytical system. The wearable nature of the wireless transceiver makes the entire device quite user friendly without compromising the ability of the sensor to monitor the sodium dynamics, in real time, in the perspiration.

#### 4. Conclusions

The article describes the fabrication, in-vitro and epidermal evaluation of a wearable tattoo sensor for continuous sodium monitoring in human perspiration. The tattoo ISE can be coupled with a Bluetooth capable wearable electronic transceiver making the entire device easily worn by an individual, obviating the need for wires for data recording. Extensive in-vitro characterization of the Na-tattoo sensor reveals that the device has a long shelf-life while maintaining its near-Nernstian response. Additionally, the Na-tattoo can survive extreme stress fatigues caused due to bending, stretching and poking. On-body testing during exercise activity demonstrated the ability of the tattoo potentiometric sensor to monitor sweat sodium dynamics via a wearable wireless transceiver. The wireless nature of the device offers complete freedom to the wearer to perform the workout bout. The Na-tattoo sensing system thus holds considerable promise as a viable device for monitoring sodium in sweat and opens up new avenues in the field of wearable wireless non-invasive sensors and body sensor networks in connection to diverse fitness, military and medical applications. Yet, several challenges, such as minimizing potential drift, integrating temperature sensor (for addressing changes in body temperature), and further miniaturization of the transceiver, need to be met before the realization of such routine real-life applications. These developments will be followed by extensive studies involving a larger population.

#### Acknowledgments

This work was supported by the National Science Foundation (Awards CBET-1066531). D.M. acknowledges support from DAAD-Promos-Programm zur Steigerung der Mobilität von deutschen Studierenden (Germany). T.G. acknowledges support from Ministry of Science and Innovation (MICINN) of Spain, Ramón y Cajal Programme, Ministry of Economy and Competitiveness, FPI fellowship (BES-2011-048297) and EEBB-I-13-05936. J.R.W. acknowledges support from UCSD von Liebig Center under the DOE-sponsored Clean Energy Technology Acceleration Program. The authors thank Kevin Chen and Wayne Neilson for assisting in the mechanical resiliency studies.

## References

- Allan, J.R., Wilson, C.G., 1971. *Journal of Applied Physiology* 30, 708–712.
- Bandodkar, A.J., Hung, V.W.S., Jia, W., Valdes-Ramírez, G., Windmiller, J.R., Martinez, A.G., Ramírez, J., Chan, G., Kerman, K., Wang, J., 2013. *Analyst* 138, 123–128.
- Bandodkar, A.J., O' Mahony, A.M., Ramírez, J., Samek, I.A., Anderson, S.M., Windmiller, J.R., Wang, J., 2013. *Analyst* 138, 5288–5295.
- Bank, S., Marks, I.N., Novis, B., 1978. *American Journal of Digestive Diseases* 23, 178–181.
- Bates, G.P., Miller, V.S., 2008. *Journal of Occupational Medicine and Toxicology* 3, 4–9.
- Buck, R.P., 1978. *Analytical Chemistry* 50, 17R–29R.
- Buono, M.J., Ball, K.D., Kolkhorst, F.W., 2007. *Journal of Applied Physiology* 103, 990–994.
- Eichner, E.R., 2008. *Current Sports Medicine Reports* 7, S36–S40.
- Fay, C., Anastasova, S., Slater, C., Buda, S.T., Shepherd, R., Corcoran, B., O'Connor, N.E., Wallace, G.G., Radu, A., Diamond, D., 2011. *IEEE Sensors Journal* 11, 2374–2382.
- Fibbioli, M., Morf, W.E., Badertscher, M., de Rooij, N.F., Pretsch, E., 2000. *Electroanalysis* 12, 1286–1292.
- Gallagher, A.J., Ni Anniadh, A., Bruyere, K., Otténio, M., Xie, H., Gilchrist, M.D., 2012. *Proc. International Research Council on the Biomechanics of Injury Conference* 40, 494–502.
- Guinovart, T., Bandodkar, A.J., Windmiller, J.R., Andrade, F.J., Wang, J., *Analyst*, DOI: 10.1039/C3AN01672B.T. Guinovart, G. A. Crespo and F. J. Andrade. Submitted
- Guinovart, T., Parrilla, M., Crespo, G.A., Rius, F.X., Andrade, F.J., 2013. *Analyst* 138, 5208–5215.
- Harvey, C.J., LeBouf, R.F., Stefaniak, A.B., 2010. *Toxicology in Vitro* 24, 1790–1796.
- Jacquemoud, C., Bruyere-Garnier, K., Coret, M., 2007. *Journal of Biomechanics* 40, 468–475.
- Jia, W., Bandodkar, A.J., Valdés-Ramírez, G., Windmiller, J.R., Yang, Z., Ramírez, J., Chan, G., Wang, J., 2013. *Analytical Chemistry* 85, 6553–6560.
- Jia, W., Valdés-Ramírez, G., Bandodkar, A.J., Windmiller, J.R., Wang, J., 2013. *Angewandte Chemie International Edition* 52, 7233–7236.

- Kim, D.H., Lu, N., Ma, R., Kim, Y.S., Kim, R.H., Wang, S., Wu, J., Won, S.M., Tao, H., Islam, A., Yu, K.J., Kim, T.I., Chowdhury, R., Ying, M., Xu, L., Li, M., Chung, H.J., Keum, H., McCormick, M., Liu, P., Zhang, Y.W., Omenetto, F.G., Huang, Y., Coleman, T., Rogers, J.A., 2011. *Science* 333 (6044), 838–843.
- Ladell, W.S.S., 1955. *Journal of Physiology* 127, 11–46.
- Lee, N.V.L., Miller, P.W., Buono, M.J., 2010. *Clinical Physiology and Functional Imaging* 30, 13–16.
- Morris, D., Schazmann, B., Wu, Y., Coyle, S., Brady, S., Fay, C., Hayes, J., Lau, K.T., Wallace, G., Diamond, D., 2008. *Conference Proceeding of IEEE Engineering in Medicine & Biology Society* 1-8, 5741–5744.
- Novell, M., Guinovart, T., Steinberg, I.M., Steinberg, M., Rius, F.X., Andrade, F.J., 2013. *Analyst* 138, 5250–5257.
- Gonzalo-Ruiz, J., Mas, R., de Haro, C., Cabruja, E., Camero, R., Alonso-Lomillo, M.A., Muñoz, F.J., 2009. *Biosensors and Bioelectronics* 24, 1788–1791.
- Rosner, M.H., Kirven, J., 2007. *Clinical Journal of the American Society of Nephrology* 2, 151–161.
- Rowell, L. B., Murray, J. A., Brengelmann, G. L., Kraning, K.K., 1969. *Circulation Research* XXIV, 711–724.
- Sato, K., Kang, W.H., Saga, K., Sato, K.T., 1989. *Journal of the American Academy of Dermatology* 20, 537–563.
- Schazmann, B., Morris, D., Slater, C., Beirne, S., Fay, C., Reuveny, R., Moyna, N., Diamond, D., 2010. *Analytical Methods* 2, 342–348.
- Sigal, C.B., Dobson, R.L., 1968. *The Journal of Investigative Dermatology* 50, 451–455.
- Speedy, D.B., Noakes, T.D., Schneider, C., 2001. *Emergency Medicine* 13, 17–27.
- Stern, R.C., 1997. *The New England Journal of Medicine* 336, 487–491.
- Taylor, H.L., Henschel, A., Mickelsen, O., Keys, A., 1943. *American Journal of Physiology* 140, 439–451.
- Windmiller, J.R., Bandodkar, A.J., Valdes-Ramírez, G., Parkhomovsky, S., Martinez, A.G., Wang, J., 2012. *Chemical Communications* 48, 6794–6796.
- Windmiller, J.R., Wang, J., 2013. *Electroanalysis* 25, 29–46.

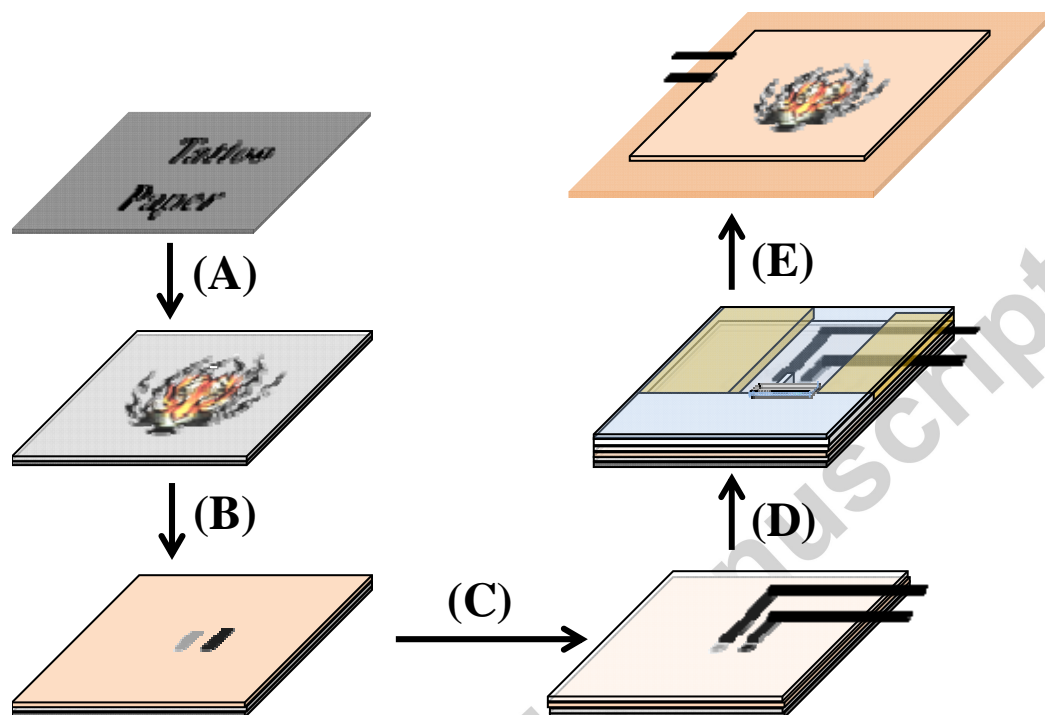


**Fig. 1:** Schematic showing the fabrication and transfer process for the Na-tattoo sensor. The first step involves (A) screen printing an insulator coating (light gray) on the tattoo paper (dark gray) followed by laser printing the “*Tiger Face*”. (B) Subsequently, a layer of skin color ink is coated and the two electrodes are screen printed. (C) Thereafter another layer of insulator (light gray) is printed to define the electrode area and contact points. For coupling the sensor to the wireless transceiver, flexible carbon coated PET connectors are attached to the printed contact points. (D) The two electrodes are then modified with respective membrane cocktails. Later the “*stick-on fluidic channel*” (details of fabrication in Fig. S1) is affixed to the Na-tattoo. (E) Finally the Na-tattoo sensor can be applied to the skin similar to any commercial temporary transfer tattoo.

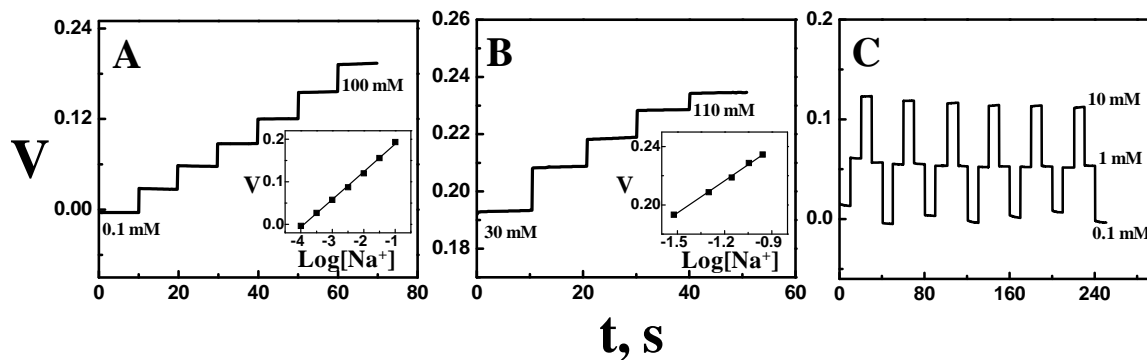


**Fig. 2:** Response of the Na-tattoo sensor to (A) NaCl solutions (0.1 – 100 mM range); (B) artificial sweat with increasing sodium concentration (30 – 110 mM). Insets show the corresponding calibration plots. (C) Carry-over study examining the dynamic response of the Na-tattoo sensor to alternating 0.1, 1 and 10 mM NaCl solutions.

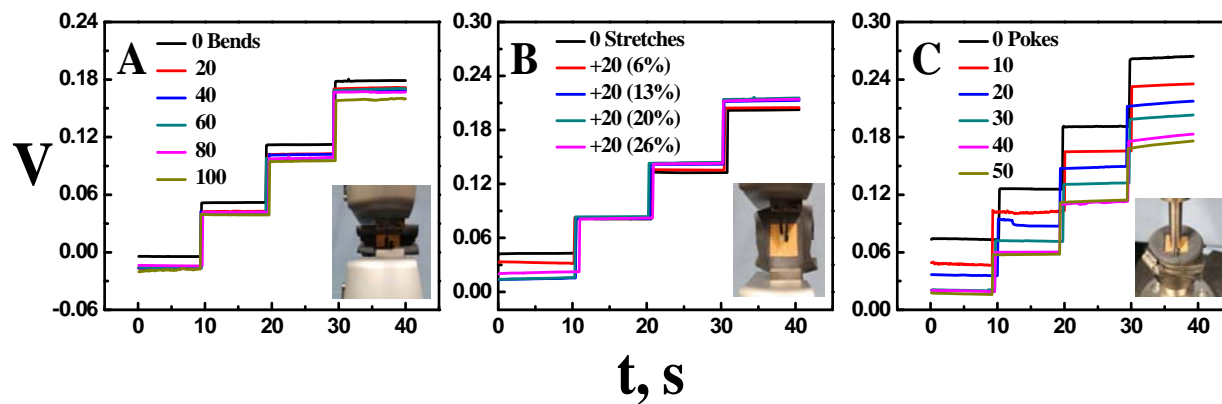


**Fig. 3:** Effect of (A) bending; (B) stretching and (C) poking stress iterations on the Na-tattoo sensor response for NaCl solutions over the 0.1 – 100 mM range. *Note:* In the stretching study, an increasing strain from 0 to 26% was applied after every 20 stretching cycles.

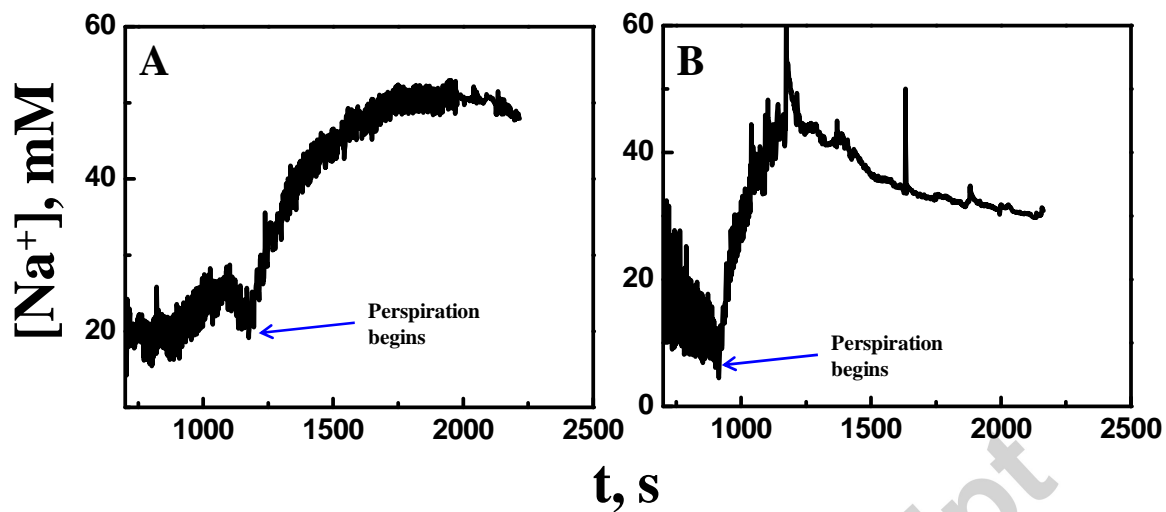


**Fig. 4:** Real-time monitoring of sodium sweat levels for two subjects over a period of 36 min (30 min exercise activity (cycling) followed by 3 min of cool down and another 3 min of complete rest) by the skin-worn Na-tattoo sensor coupled with an electrochemical analyzer.

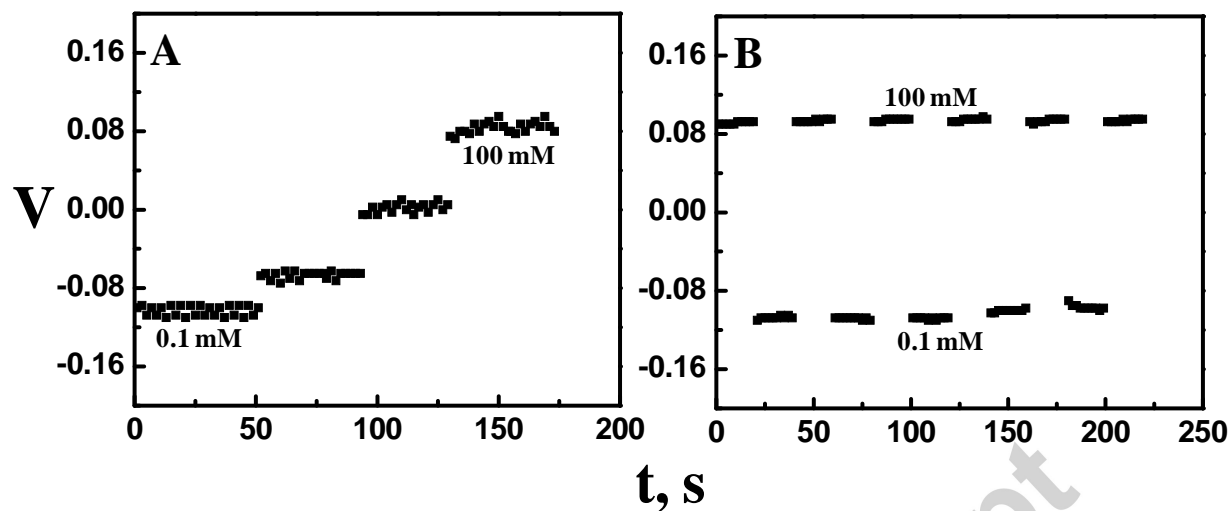


**Fig. 5:** Wirelessly transmitted analytical sensor response (A) for NaCl solutions of varying concentrations (0.1 – 100 mM) and (B) during carry-over study using 0.1 and 100 mM NaCl solutions.

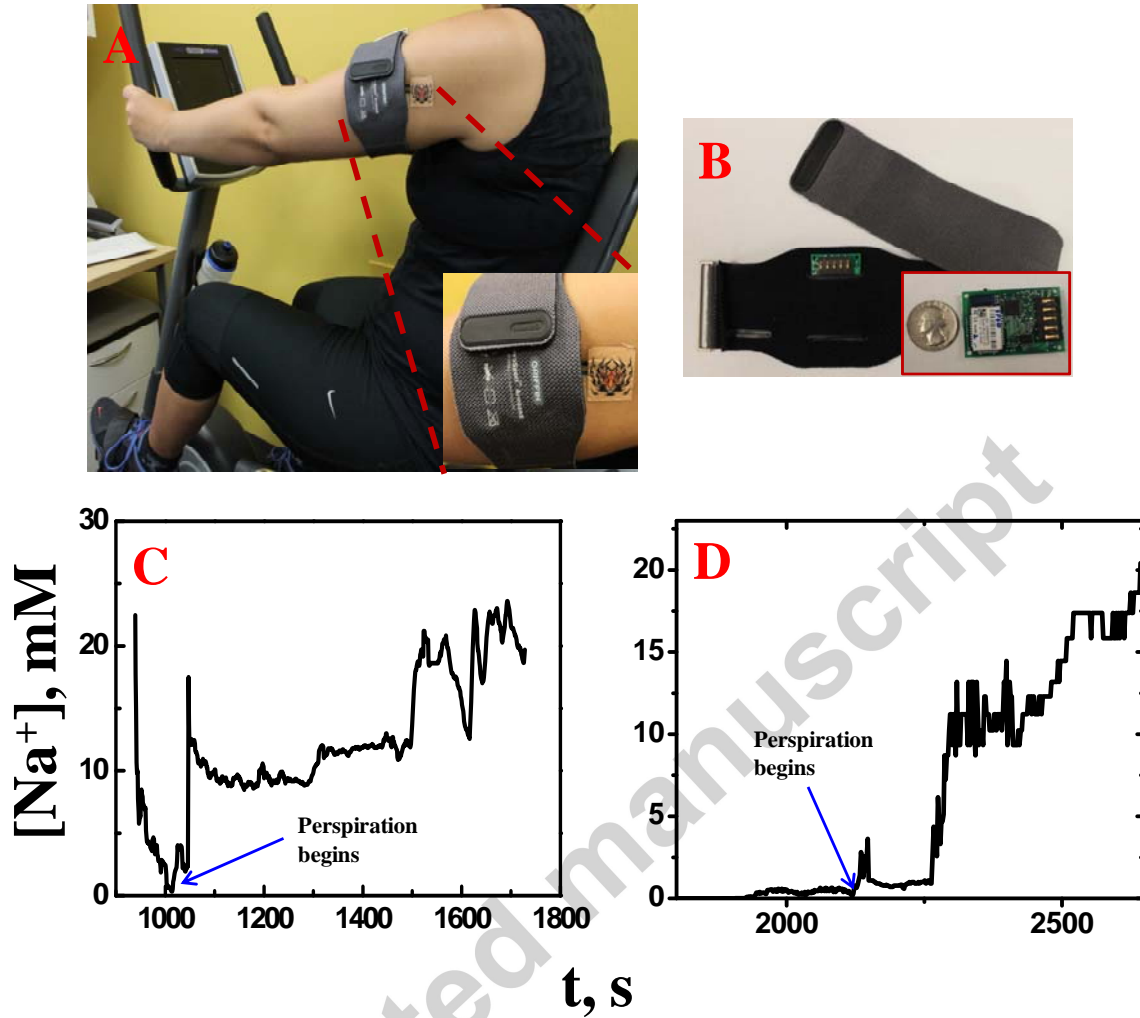


**Fig. 6:** Photographs of wireless transceiver (A) worn by a subject along with the Na-tattoo (inset: a zoomed image of the entire device); (B) when encapsulated in an armband (inset: image showing a quarter dollar kept close to wireless transceiver for size comparison and (C, D) Real-time sodium concentration monitoring in sweat by the Na-tattoo coupled with the wireless transceiver for two different subjects.